Convergence of a cartesian method for interface elliptic problems

Lisl Weynans[0000−0003−0376−8747]

Abstract We study the convergence of a Cartesian method for elliptic problems with immersed interfaces. This method is based on additional unknowns located on the interface, used to express the jump conditions across the interface and discretize the elliptic operator in each subdomain separately. It is numerically second-order accurate in L^∞-norm. We prove the convergence of the method in two cases: the original second-order method in one dimension, and a first-order version in two dimensions. The proof of convergence takes advantage of a discrete maximum principle to obtain estimates on the coefficients of the inverse matrix. More precisely, we obtain estimates for the sums of the coefficients of several blocks of the inverse matrix. Associated to the consistency error, which has different leading orders throughout the domain, these estimates lead to the convergence results. The methodology exposed in the article allows to take into account the effects of different orders of approximation errors across the domain and their effective influence on the total convergence order.

1 Introduction

In this paper we aim to study the convergence of a method for solving an elliptic problem on a Cartesian grid. This elliptic problem is defined on a domain Ω consisting in the union of two subdomains Ω_1 and Ω_2, separated by a complex interface Σ (see Figure 1):

$$-\nabla.(k\nabla u) = f \text{ on } \Omega = \Omega_1 \cup \Omega_2, \tag{1}$$

$$u_2 - u_1 = \alpha \text{ on } \Sigma, \tag{2}$$

$$k_2 \frac{\partial u_2}{\partial n} - k_1 \frac{\partial u_1}{\partial n} = \beta \text{ on } \Sigma, \tag{3}$$

Lisl Weynans
Univ. Bordeaux, France., e-mail: lisl.weynans@math.u-bordeaux.fr

assorted with Dirichlet boundary conditions on $\delta\Omega$, defined as the boundary of Ω. The notations u_1, u_2 and k_1, k_2 refer respectively to the restrictions of u and k to the subdomains Ω_1 and Ω_2, k being a constant on each subdomain Ω_1 and Ω_2. The domain Ω can have an arbitrary shape. In the whole paper, we assume that the interface is C^2 and that the solution u of problem (1)-(3) exists and is smooth enough so that our truncation error analyses are valid. We assume, by convention, that the coefficient k is larger in Ω_2 than in Ω_1 ($k_2 > k_1$), and that the vector $\boldsymbol{n}$ is the outward normal for the subdomain Ω_2. Note that other configurations than the one illustrated in this figure are possible, for instance, Ω_1 separated in several subdomains, and are all covered by our analysis.

This elliptic problem with discontinuities across an interface appears in numerous physical or biological models. Among the well-known applications are heat transfer, electrostatics, incompressible flows with discontinuous densities and viscosities [4], but similar elliptic problems arise for instance in tumour growth modelling, where one has to solve a pressure equation [8], or in the modelling of electric potential in biological cells: see for instance [9] or [23] and [24] where the mentioned numerical method was applied.

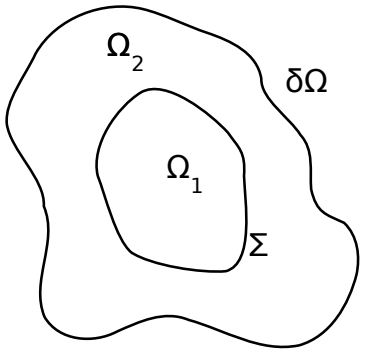

Fig. 1 Geometry considered: two subdomains Ω_1 and Ω_2 separated by a complex interface Σ.

The method that we study was developed in [12]. It is based on a finite-difference discretization and a dimension by dimension approach. In order to solve accurately the problem defined by equations (1) - (3) near the interface, additional unknowns are defined at the intersections of the interface with the grid, see Figure 2. These interface unknowns are used in the discretization of the elliptic operator near the interface. In order to solve the interface unknowns, the flux jump conditions are discretized and added to the linear system to solve.

This approach has the following advantages: firstly, the use of unknowns avoids the need to devise specific formulas containing jump terms, corrective terms, or needing

the inversion of a linear system, for discretising the operator near the interface. Secondly, it is flexible, in the sense that it can easily be adapted to an elliptic problem whose conditions at the interface are different from the one presented in this article. Finally, for a number of applied problems, as incompressible mutlifluids or electropermeabilization of biological cells for example), it may be useful to know the values of certain unknowns directly at the interface, which is possible without any additional calculations using the method presented here.

In the following we will prove the convergence of the method in two cases: the original second-order method in one dimension, and a first-order version in two dimensions. This first-order version is based on the same ideas as the original method, but the discretization of the normal derivatives across the interface has only a first-order truncation error instead of a second-order for the original method. This variant has recently been used to discretize fluxes in [14] for an electrical impedance tomography problem.

The convergence proof is based on a discrete maximum principle, used to provide estimates of the coefficients of the inverse of the discretization matrix. To this purpose we have to prove the monotonicity of the discretization matrix. This monotonicity property is not straightforward for the second-order discretization, since the discretization matrix is not diagonally dominant, due to the discretization of the flux jump conditions across the interface.

Then we obtain accurate estimates of the coefficients of the inverse matrix, block by block, in order to account for the different types of truncation errors. Combined to the truncation error expressed block by block, these estimates provide first- or second-order bounds on the numerical error.

In section 2 we describe the numerical schemes, in section 3 and 4 we present the proof for the first-order version in two dimensions and the second-order version in one-dimension. In section 5 we compare our approach to the literature and in section 6 we present some numerical tests corroborating our analysis.

2 Description of the numerical schemes

2.1 Interface representation and classification of grid points

In order to describe accurately the geometric configuration in the vicinity of the interface we use the level set method introduced by Osher and Sethian [33]. We refer the interested reader to [34], [35] and [32] for reviews of this method. We recall here some properties that we will use in the following.

- The zero isoline of the level set function, defined here by the signed distance function ϕ:

$$\phi(x) = \begin{cases} dist_\Sigma(x) & \text{outside of the interface,} \\ 0 & \text{on the interface,} \\ -dist_\Sigma(x) & \text{inside of the interface,} \end{cases} \tag{4}$$

implicitly represents the interface Σ immersed in the computational domain.

- As recalled in [13], the level-set, being a distance function, is 1-Lipshitz and almost everywhere differentiable. Moreover, if ϕ is differentiable at a point x, then it satisfies the so-called Eikonal equation at x:

$$||\nabla\phi(x)|| = 1.$$

- The smoothness of the level-set is in fact strongly related to the smoothness of the interface: as proved in [19], p 355, if the interface is C^2, then there exists a real $r_0 > 0$ such that the level-set is C^2 for all x, y such that $|\phi(x, y)| < r_0$.
- The outward normal vector of the isoline of ϕ passing through x, denoted $\boldsymbol{n}(x)$, can be expressed, where ϕ is differentiable, as

$$\boldsymbol{n}(x) = \frac{\nabla\phi(x)}{|\nabla\phi(x)|}. \tag{5}$$

  In this paper, the level-set is defined so that $\boldsymbol{n}$ is the outside normal for the subdomain Ω_2.

The problem (1) - (3) is discretized on a uniform Cartesian grid covering $\Omega_1 \cup \Omega_2$, see Figure 2. The grid spacing is denoted h. The points on the cartesian grid are named either with letters such as P or Q, or with indices such as $M_{i,j} = (x_i, y_j) = (i\,h, j\,h)$ if one needs to have informations about the location of the point. We also denote if more convenient x_P and y_P the coordinates of a point P. We denote by u_{ij}^h or u_M^h the approximation of u at the point $M = (x_i, y_j)$. The set of grid points located inside the domain Ω is denoted Ω_h.

We say that a grid point is irregular if the sign of ϕ changes between this point and at least one of its neighbors, see Figure 2. On the contrary, grid points that are not irregular are called regular grid points. The set of irregular grid nodes is denoted Ω_h^*. The subset Ω_h^δ is defined as the set of regular grid points where the stencil for the discrete elliptic operator (described in the following) crosses the isolines $\phi = \delta$ or $\phi = -\delta$, with δ such that $0 < \delta < r_0$. Notably ϕ is C^2 on Ω_h^δ with bounded derivatives.

We define the interface point $I_{i+1/2,j} = (x_{i+1/2,j}, y_j)$ as the intersection of the interface and the segment $[M_{ij}M_{i+1j}]$, if it exists. Similarly, the interface point $I_{i,j+1/2} = (x_i, y_{i,j+1/2})$ is defined as the intersection of the interface and the segment $[M_{ij}M_{ij+1}]$. The set of interface points is denoted Σ_h, see Figure 2 for an illustration. At each interface point we create two additional unknowns, called interface unknowns, and denoted by $u_{i+1/2,j}^{1,h}$ and $u_{i+1/2,j}^{2,h}$, or $u_{i,j+1/2}^{1,h}$ and $u_{i,j+1/2}^{2,h}$. The interface unknowns carry the values of the numerical solution on each side of the interface.

We also denote $\delta\Omega_h$ the set of points defined as the intersection between the grid and $\delta\Omega$. They are used to impose Dirichlet boundary conditions.

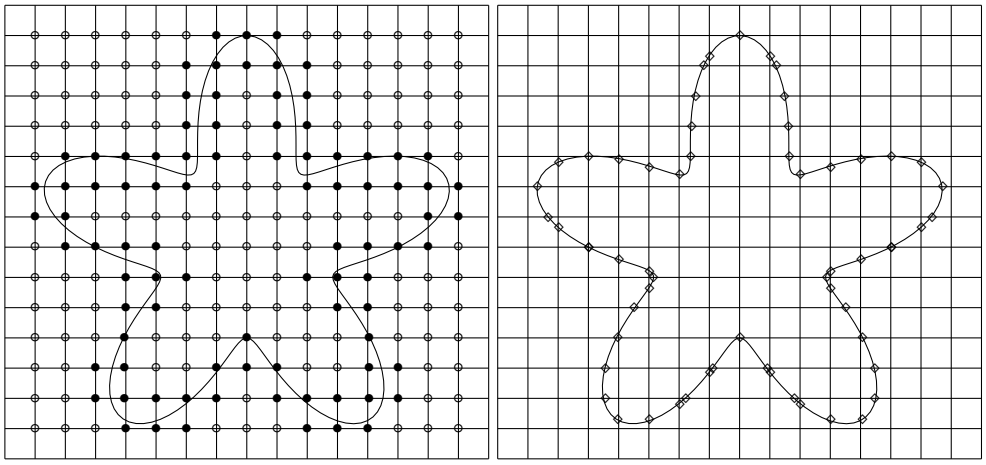

Fig. 2 Left: regular nodes described by circles ∘, irregular nodes (belonging to Ω_h^*) described by bullets •, right: nodes belonging to Σ_h.

2.2 Second-order discretization in one dimension

We recall here the discretization presented in [12] applied in one dimension.

- Discrete elliptic operator on a grid point M_i
  We use the standard three point stencil: M_i and its nearest neighbors in each direction, either grid or interface points. We denote u_E (resp. u_W) the value of the numerical solution on the nearest point in the east (resp. west) direction, and x_E (resp. x_w) its coordinate. The discretization at point M_i reads

$$-\Big(\nabla.(k\nabla u)\Big)_i^h = -k_i \frac{2}{x_E - x_W}\Big(\frac{u_E - u_i}{x_E - x_i} - \frac{u_i - u_W}{x_i - x_W}\Big). \tag{6}$$

  The truncation error of this discretization is second-order accurate on regular points, and first-order otherwise.
- Discrete jump conditions across the interface
  On Figure 3, we present a prototypical situation around the interface: the interface point, whose coordinate is $x_{int} = x_{k+1/2}$, is located between the grid points corresponding to coordinates x_k and x_{k+1} and we denote $dh = x_{k+1} - x_{k+1/2}$. We assume for instance that the subdomain Ω_2 is located on the left side of the interface, and Ω_1 on the right side. The normal to the interface is oriented from the left to the right.
  The left and right normal derivatives at the interface are computed with second-order formulas using three non-equidistant points:

$$(\partial_n u^1)^h_{k+1/2} = \frac{1+2d}{d(d+1)h}(u^h_{k+1} - u^{1,h}_{k+1/2}) - \frac{d}{(1+d)h}(u^h_{k+2} - u^h_{k+1}),$$
$$(\partial_n u^2)^h_{k+1/2} = \frac{3-2d}{(1-d)(2-d)h}(u^{2,h}_{k+1/2} - u^h_k) - \frac{1-d}{(2-d)h}(u^h_k - u^h_{k-1}).$$

We express the jump conditions at point $x_{k+1/2}$ as

$$u^{2,h}_{k+1/2} - u^{1,h}_{k+1/2} = \alpha(x_{k+1/2}), \tag{7}$$
$$k_2(\partial_n u^2)^h_{k+1/2} - k_1(\partial_n u^1)^h_{k+1/2} = \beta(x_{k+1/2}). \tag{8}$$

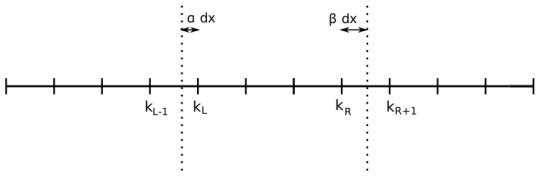

Fig. 3 Geometrical configuration near the interface in one dimension.

2.3 First-order discretization in two dimensions

We present here the variant of the method of [12] with the jump on the fluxes discretized with a first-order accuracy.

- Discrete elliptic operator
  We use a standard five point stencil with the grid point $M_{i,j}$ and its nearest neighbors, interface or grid points, in each direction. More precisely, we denote u^h_S the value of the solution on the nearest point in the south direction, with coordinates (x_S, y_S). Similarly, we define u^h_N, u^h_W and u^h_E and the associated coordinates (x_N, y_N), (x_W, y_W) and (x_E, y_E). The discretization reads

$$\begin{aligned} -\Big(\nabla.(k\nabla u)\Big)^h_{i,j} &= -\Big(\nabla.(k\nabla u)\Big)^h(x_i, y_j), \\ &= -k_{i,j}\Big(\frac{u^h_N - u^h_{ij}}{x_N - x_i} - \frac{u^h_{ij} - u^h_S}{x_i - x_S}\Big)\frac{2}{x_N - x_S} \\ &\quad -k_{i,j}\Big(\frac{u^h_E - u^h_{ij}}{y_E - y_j} - \frac{u^h_{ij} - u^h_W}{y_j - y_W}\Big)\frac{2}{y_E - y_W}. \end{aligned} \tag{9}$$

  The truncation error of this discretization is second-order accurate on regular grid points, and first-order on irregular grid points.
- Discrete jump conditions across the interface

We discretize the jump conditions (2) and (3) at each interface point $I_{i+1/2,j}$ as:

$$u^{2,h}_{i+1/2,j} - u^{1,h}_{i+1/2,j} = \alpha(I_{i+1/2,j}), \tag{10}$$

$$k_2(\partial_n u^2)^h_{i+1/2,j} - k_1(\partial_n u^1)^h_{i+1/2,j} = \beta(I_{i+1/2,j}), \tag{11}$$

and similarly for each interface point $I_{i,j+1/2}$. The discretization of the normal derivatives depends on the local geometry of the interface. On Figure 4 one can observe the four possible cases that are met if h is small enough. The first intersection between the normal to the interface and the grid is located on a segment: either $[M_{i,j-1}, M_{i,j}]$, or $[M_{i,j-1}, M_{i+1,j-1}]$, or $[M_{i,j}, M_{i,j+1}]$, or $[M_{i,j+1}, M_{i+1,j+1}]$.

The discrete normal derivative is computed as the normal derivative of the linear interpolant of the numerical solution on the triangle composed of the interface point $I_{i+1/2,j}$ and the aforementioned segment. If we denote K this triangle, (x_1, y_1), (x_2, y_2) and (x_3, y_3) its vertices, and u_1, u_2 and u_3 the associated values, the basis functions on the vertices for the linear interpolation write

$$\lambda_j(x, y) = \alpha_j x + \beta_j y + \gamma_j, \;\; j = 1, 2, 3,$$

with

$$\alpha_j = \frac{y_k - y_i}{(x_j - x_k)(y_j - y_i) - (x_j - x_i)(y_i - y_k)},$$
$$\beta_j = \frac{x_i - x_k}{(x_j - x_k)(y_j - y_i) - (x_j - x_i)(y_i - y_k)},$$
$$\gamma_j = \frac{x_k y_i - x_i y_k}{(x_j - x_k)(y_j - y_i) - (x_j - x_i)(y_i - y_k)},$$

(n_x, n_y) being an approximation of the normal at the interface point. With these notations, the approximation of the normal derivative writes for instance for the interface point $I_{i+1/2,j}$

$$(\partial_n u)^h_{i+1/2,j} = (u_1\,\alpha_1 + u_2\,\alpha_2 + u_3\,\alpha_3)n_x + (u_1\,\beta_1 + u_2\,\beta_2 + u_3\,\beta_3)n_y.$$

This discretization is only first-order accurate because it is based on a linear interpolation.

2.4 Elimination of the interface values on the Ω_2 side

We replace the variables $u^{2,h}_{i+1/2,j}$ and $u^{2,h}_{i,j+1/2}$ by $u^{1,h}_{i+1/2,j} + \alpha(I_{i+1/2,j})$ and $u^{1,h}_{i,j+1/2} + \alpha(I_{i,j+1/2})$ in the equations (8) or (11), and (6) or (9), in order to eliminate the jump conditions (10) or (7) from the linear system. Because the jump conditions (7) or (10) are expressed exactly, this does not change the truncation errors. In the following we denote A_h the matrix of the linear system resulting from this discretization. The local

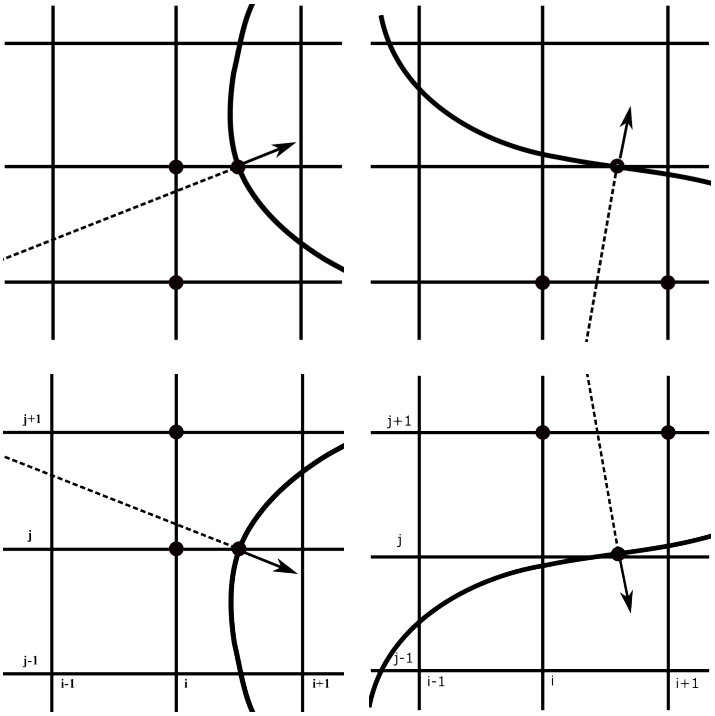

Fig. 4 All possible stencils for the first-order flux discretization on the left side of the interface, with points involved in the discretization signaled by black circles.

error array $\mathbf{e_h}$ and the consistency error array $\tau_\mathbf{h}$ obey the same linear relationship as the numerical solution and the source terms:

$$A_h \mathbf{e_h} = \tau_\mathbf{h}.$$

Due to the discretization that we have chosen, the truncation error amplitude is:

- for the first-order version in two-dimensions: $O(h^2)$ on regular grid points, $O(h)$ on irregular grid points, and $O(h)$ on interface points,
- for the second-order version in one-dimension: $O(h^2)$ on regular grid points, $O(h)$ on irregular grid points, and $O(h^2)$ on interface points.

For the sake of simplicity we assume that the boundary conditions on $\delta\Omega$ are Dirichlet boundary conditions imposed exactly. Consequently, the local error $\mathbf{e}$ is zero on $\delta\Omega_h$.

3 Convergence proof in two dimensions for the first-order version of the method

First we prove the monotonicity of the discretization matrix, then we use it to apply a discrete maximum principle to the matrix, and obtain estimates on the coefficients of the inverse matrix, block by block.

3.1 Monotonicity of the discretization matrix

Here we aim to prove that A_h is monotone, that is, that all the coefficients of the inverse matrix of A_h are non-negative. To prove this result, we use the following lemma:

Lemma 1 *With the convention used for the normal to the interface, illustrated on Figure 5, if the minimum of v is located on an interface point, then at this interface point the discrete normal derivative in Ω_1 is positive and the discretized normal derivative in Ω_2 is negative.*

Proof. The approximation of the normal derivative is constant, because it is computed from a linear interpolation on a triangle. If the minimum of v is located on the considered interface point, then the left normal derivative at this interface point is negative and the right normal derivative at this interface point is positive. Moreover, if the minimum of v is located on an interface point, and if the approximated normal derivative at this point is zero, then the three points values involved in the stencil are equal. □

Theorem 1 *Let v be an array of size $N + N_{int}$, corresponding to N grid points and N_{int} interface unknowns, such that all coefficients of $A_h v$ are non-negative, which we denote $A_h v \geq 0$, A_h being the discretization matrix corresponding of the method in two-dimensions described in subsection 2.3.*

Then, all coefficients of v are non-negative.

Before presenting the proof, let us remark that this property also means that A_h is invertible. Indeed, let us assume that an array v is such that $A_h v = 0$. It means that both $A_h v$ and $A_h(-v)$ are non-negative. Consequently, we have $v \geq 0$ and $-v \geq 0$, thus $v = 0$.

Proof. Let v be an array of size $N + N_{int}$, corresponding to N grid points and N_{int} interface unknowns, such that all coefficients of $A_h v$ are non-negative, which we denote $A_h v \geq 0$.

We consider the minimum of v in the whole domain, interface points included. This value can either be located on a grid point in one of the subdomains Ω_1 or Ω_2, or on an interface point.

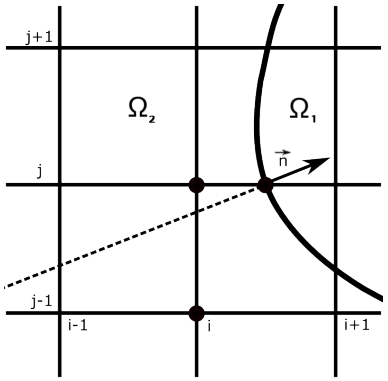

Fig. 5 Geometrical configuration near the interface in two dimensions.

- If the minimum is located on one border of the computational domain
  We assume for instance that the minimum of v is $v_{1,j}$, located on the grid point $M_{1,j}$, such that $M_{2,j}$, $M_{1,j+1}$ and $M_{1,j-1}$ also belong to the computational domain. Therefore, the boundary is located on the left side of $M_{1,j}$. The other cases would be treated the same way. The elliptic operator inequality on this grid point yields:

$$\frac{4v_{1,j} - v_{2,j} - v_{1,j+1} - v_{1,j-1}}{h^2} \geq 0,$$

  then we have $4v_{1,j} \geq v_{2,j} + v_{1,j+1} + v_{1,j-1} \geq 3v_{1,j}$ and thus $v_{1,j} \geq 0$. Therefore all values of v are non-negative.
- If the minimum is reached on a grid point in one subdomain sharing at least one point with $\delta\Omega$
  In this case we denote (i_0, j_0) the indices of the smallest component of v. We assume the grid point is a regular grid point (otherwise the formula would have slightly different weights, but the reasoning would be the same). Using the elliptic operator inequality on this point we can write:

$$4v_{i_0,j_0} - v_{i_0+1,j_0} - v_{i_0-1,j_0} - v_{i_0,j_0+1} - v_{i_0,j_0-1} \geq 0,$$

  we deduce that $v_{i_0+1,j_0} = v_{i_0-1,j_0} = v_{i_0,j_0+1} = v_{i_0,j_0-1} = v_{i_0,j_0}$. Repeating this reasoning on the neighbours of (i_0, j_0), then on the neigbours of the neighbours etc, we deduce that all values in the subdomain, including the boundary values, are equal to v_{i_0,j_0}. We use now the reasoning of the last paragraph to conclude that all values of v are non-negative.
- If the minimum is reached on a grid point in one subdomain which does not share any point with $\delta\Omega$
  We use the notations and geometrical configuration of Figure 5. We assume, without loss of generality, that the subdomain is Ω_1 and we denote (i_0, j_0) the indices of the minimum of v. With the same reasoning as in the previous paragraph, we can prove that all values in the subdomain, including the interface values, are equal to the minimum value v_{i_0,j_0}.

Let us consider one of these interface values, located for instance on point $I_{i+1/2,j}$. As noticed previously, the fact that all values are equal in the subdomain implies that the normal derivative at the interface point is zero. Due to the fact that $A_h v \geq 0$, we can write on this interface point:

$$0 = k_1(\partial_n v^1)^h_{i+1/2,j} \leq k_2(\partial_n v^2)^h_{i+1/2,j}.$$

On the other side, because the minimum value is reached on this interface point, we also have

$$(\partial_n v^2)^h_{i+1/2,j} \leq 0.$$

Consequently, $(\partial_n v^1)^h_{i+1/2,j} = (\partial_n v^2)^h_{i+1/2,j} = 0$, and the values of the grid points involved in the stencil for $(\partial_n v^2)^h_{i+1/2,j}$ are equal to the value of the interface point. It means that there are two grid points in the subdomain Ω_2 where the minimum value is reached.
In this paper we have considered so far that there are only two subdomains. Therefore, we know that the subdomain Ω_2 has a non-void intersection with $\delta\Omega$, and we use the reasoning of the previous paragraph to conclude. In the case where more subdomains were considered, we would distinguish whether the subdomain Ω_2 has a non-void intersection with $\delta\Omega$ or not. If not the case, then we would apply again the reasoning of this paragraph, switching from subdomains to subdomains, until finding a subdomain whose intersection with $\delta\Omega$ is non empty.

- If the minimum is located on one interface point
Without loss of generality, we assume that the minimum is located on $I_{i+1/2,j}$. On this interface point we have the two relationships

$$(\partial_n v^2)^h_{i+1/2,j} \leq 0,$$
$$(\partial_n v^1)^h_{i+1/2,j} \geq 0.$$

Furthermore, we know that

$$k_2(\partial_n v^2)^h_{i+1/2,j} - k_1(\partial_n v^1)^h_{i+1/2,j} \geq 0.$$

We infer from the previous inequalities that $(\partial_n v^2)^h_{i+1/2,j} = (\partial_n v^1)^h_{i+1/2,j} = 0$. Therefore there are at least two grid points in each subdomain where the minimum value is reached. We can then follow the reasoning of one of the two last paragraphs.

We have proven that if $A_h v$ is non-negative, then v is also non-negative. □

3.2 Discrete Green functions

In the following, the letters P and Q represent either discretization points (on the grid or on the interface) or their indices in the global numbering of the matrix. For instance, we denote $u(P)$ the coefficient of the row of u with the same index than the point P. Similarly, $A_h U(P)$ represents the coefficient of the P-th row of the array $A_h U$, and $A_h(P,Q)$ is the coefficient of the P-th row and Q-th column of the matrix A_h. We also define respectively by $A_h(:,Q)$ and $A_h(P,:)$ the Q-th column and the P-th row of the matrix A_h.

For each $Q \in \Omega_h \cup \Sigma_h$, define the discrete Green's function $G_h(:,Q) = \Big(G_h(P,Q)\Big)_{P \in \Omega_h \cup \Sigma_h \cup \delta\Omega_h}$ as the solution of the discrete problem:

$$\begin{cases} A_h G_h(:,Q)(P) = \begin{cases} 0, & P \neq Q \\ 1, & P = Q \end{cases} & P \in \Omega_h \cup \Sigma_h, \\ G_h(P,Q) = 0, & P \in \delta\Omega_h. \end{cases} \tag{12}$$

The matrix A_h being monotone, all values of $G_h(:,Q)$ are positive. For homogeneous Dirichlet boundary conditions we can write the solution of the numerical problem as a sum of the source terms multiplied by the values of the discrete Green function:

$$u_h(P) = \sum_{Q \in \Omega_h \cup \Sigma_h} G_h(P,Q)\,(A_h u_h)(Q), \quad \forall P \in \Omega_h \cup \Sigma_h.$$

The local error $e_h(P)$ can similarly be expressed as a sum of the truncation error terms multiplied by the values of the discrete Green function:

$$e_h(P) = \sum_{Q \in \Omega_h \cup \Sigma_h} G_h(P,Q)\,(\tau_h)(Q), \quad \forall P \in \Omega_h \cup \Sigma_h.$$

Now we present the result of Ciarlet in [11], based on a discrete maximum principle, slightly modified to be adapted to our discretization matrix.

Theorem 2 *Let S be a subset of points, W a discrete function with $W \equiv 0$ on $\delta\Omega_h$, i an integer and $M > 0$ a real value such that:*

$$\begin{cases} (A_h W)(P) \geq 0 & \forall P \in \Omega_h \cup \Sigma_h, \\ (A_h W)(P) \geq M^{-i} & \forall P \in S. \end{cases}$$

Then

$$\sum_{Q \in S} G_h(P,Q) \leq M^i W(P), \quad \forall P \in \Omega_h \cup \Sigma_h.$$

Proof. Using the definition of the discrete Green function, we can write

$$\Big(A_h \sum_{Q \in S} G_h(:,Q)\Big)(P) = \begin{cases} 1 & \text{if } P \notin S, \\ 0 & \text{if } P \in S. \end{cases}$$

Therefore,

$$A_h\Big(W - M^{-i}\sum_{Q\in S} G_h(:,Q)\Big)(P) \geq 0, \quad \forall P \in \Omega_h \cup \Sigma_h.$$

As all coefficients of the inverse of A_h are non-negative, it leads to

$$W(P) - M^{-i}\sum_{Q\in S} G_h(P,Q) \geq 0, \quad \forall P \in \Omega_h \cup \Sigma_h,$$

and finally we obtain an estimate of $\sum_{Q\in S} G_h(:,Q)$ in terms of the coefficients of W:

$$\sum_{Q\in S} G_h(P,Q) \leq M^i W(P), \quad \forall P \in \Omega_h \cup \Sigma_h.$$

□

This result can be generalized to several subsets, with both positive and negative lower bounds, as was proved in [14]. This allows to obtain coupled estimates between different subsets, based on discrete functions satisfying weaker assumptions.

Theorem 3 *Let S and $\tilde{S}$ be two subsets of points, W a discrete function with $W \equiv 0$ on $\delta\Omega_h$, i and j integers, and $M > 0$, $\tilde{M} > 0$ real values such that:*

$$\begin{cases} (A_h W)(P) \geq 0, & \forall P \in \Omega_h \cup \Sigma_h \setminus \tilde{S}, \\ (A_h W)(P) \geq M^{-i}, & \forall P \in S, \\ (A_h W)(P) \geq -\tilde{M}^{-j}, & \forall P \in \tilde{S}. \end{cases}$$

Then

$$\sum_{Q\in S} G_h(P,Q) \leq M^i W(P) + M^i\tilde{M}^{-j}\sum_{Q\in\tilde{S}} G_h(P,Q), \quad \forall P \in \Omega_h \cup \Sigma_h.$$

Proof. Using the definition of the discrete Green functions, we can write

$$A_h W(P) \geq A_h\Big(M^{-i}\sum_{Q\in S} G_h(:,Q) - \tilde{M}^{-j}\sum_{Q\in\tilde{S}} G_h(:,Q)\Big)(P), \quad \forall P \in \Omega_h \cup \Sigma_h.$$

As all coefficients of A_h^{-1} are non-negative, it leads to

$$W(P) - M^{-i}\sum_{Q\in S} G_h(P,Q) + \tilde{M}^{-j}\sum_{Q\in\tilde{S}} G_h(P,Q) \geq 0, \quad \forall P \in \Omega_h \cup \Sigma_h,$$

and finally we obtain the following bound:

$$\sum_{Q\in S} G_h(P,Q) \leq M^i W(P) + M^i\tilde{M}^{-j}\sum_{Q\in\tilde{S}} G_h(P,Q), \quad \forall P \in \Omega_h \cup \Sigma_h.$$

□

3.3 Convergence proof

Here we aim to obtain estimates for $\sum_{Q\in\Sigma_h} G_h(:,Q)$, $\sum_{Q\in\Omega_h} G_h(:,Q)$ and $\sum_{Q\in\Omega_h^*} G_h(:,Q)$, corresponding respectively to blocks of interface points, grid points and irregular grid points. These estimates are used to compute the convergence rate of the method.

3.3.1 Estimates for blocks of grid points and interface points

We consider the exact solution $\bar{u}$ of system (1)-(3), with $f = 1$, $\alpha = 0$, $\beta = 1$ and $u = 0$ on $\delta\Omega$. We assume that Ω and Γ are smooth enough so that $\bar{u}$ exists and is smooth enough for our analysis. By applying a maximum principle we know that $\bar{u}$ is positive on Ω.

We define the array $\bar{W}$ as the discretisation of $\bar{u}$ on the grid and interface points, with $\bar{W} \equiv 0$ on $\delta\Omega_h$. The discretization of the elliptic operator and the fluxes is consistent at least with first-order accuracy, thus for h small enough, we can write that

$$\begin{aligned}
-\Big(\nabla.(k\nabla\bar{W})\Big)^h_{i,j} &\geq \frac{1}{2}, \quad \forall M_{i,j} \in \Omega_h,\\
k_2(\partial_n\bar{W}^2)^h_{i+1/2,j} - k_1(\partial_n\bar{W}^1)^h_{i+1/2,j} &\geq \frac{1}{2}, \quad \forall I_{i+1/2,j} \in \Sigma_h,\\
k_2(\partial_n\bar{W}^2)^h_{i,j+1/2} - k_1(\partial_n\bar{W}^1)^h_{i,j+1/2} &\geq \frac{1}{2}, \quad \forall I_{i,j+1/2} \in \Sigma_h.
\end{aligned}$$

This can be rewritten as:

$$\begin{aligned}
(A_h\bar{W})(P) &\geq \frac{1}{2}, \quad \forall P \in \Omega_h,\\
(A_h\bar{W})(P) &\geq \frac{1}{2}, \quad \forall P \in \Sigma_h,
\end{aligned}$$

and using Theorem (2), it leads to:

$$\sum_{Q\in\Omega_h} G_h(:,Q) + \sum_{Q\in\Sigma_h} G_h(:,Q) \leq 2\bar{W}. \tag{13}$$

Therefore we obtain:

$$\sum_{Q\in\Sigma_h} G_h(:,Q) \leq O(1), \tag{14}$$

$$\sum_{Q\in\Omega_h} G_h(:,Q) \leq O(1). \tag{15}$$

3.3.2 Estimates for blocks of grid points in Ω_h^*

- Let $P = M_{i_0,j_0}$ be a grid point belonging to Ω_h^δ. We consider the function

$$\tilde{F}_P(x,y) = \ln(\frac{C}{r_P(x,y)}),$$

with $r_P(x,y) = \sqrt{(x-x_{i_0})^2 + (y-y_{j_0})^2 + h^2}$, and C such that $\tilde{F}_P(x,y) > 0$ for all $(x,y) \in \Omega$.
Without loss of generality, we assume in the following that $x_{i_0} = y_{j_0} = 0$. We can prove that for every regular grid point $M_{i,j}$

$$-\Big(\nabla.(k\nabla\tilde{F}_P)\Big)_{i,j}^h \geq 0, \tag{16}$$

and in particular, for the point P itself,

$$-\Big(\nabla.(k\nabla\tilde{F}_P)\Big)_{i_0,j_0}^h \geq \frac{C_1}{h^2}, \tag{17}$$

with C_1 a strictly positive constant.

Proof. On a regular grid point we can write:

$$-\Big(\nabla.(k\nabla\tilde{F}_P)\Big)_{i,j}^h = \frac{k}{h^2}\ln\Big(\frac{r_{i-1,j}\,r_{i+1,j}\,r_{i,j-1}\,r_{i,j+1}}{r_{i,j}^4}\Big) = \frac{k}{2h^2}\ln\Big(\frac{r_{i-1,j}^2\,r_{i+1,j}^2\,r_{i,j-1}^2\,r_{i,j+1}^2}{r_{i,j}^8}\Big),$$

$$= \frac{k}{2h^2}\ln\Big(\frac{\Big[(x_i+h)^2+y_j^2+h^2\Big]\Big[(x_i-h)^2+y_j^2+h^2\Big]\Big[x_i^2+(y_j+h)^2+h^2\Big]\Big[x_i^2+(y_j-h)^2+h^2\Big]}{(x_i^2+y_j^2+h^2)^4}\Big).$$

Moreover,

$$\Big[(x_i+h)^2+y_j^2+h^2\Big]\Big[(x_i-h)^2+y_j^2+h^2\Big] = (x_i^2+y_j^2+h^2)^2 + 3h^4 - 2h^2x_i^2 + 2h^2y_j^2,$$
$$\Big[x_i^2+(y_j+h)^2+h^2\Big]\Big[x_i^2+(y_j-h)^2+h^2\Big] = (x_i^2+y_j^2+h^2)^2 + 3h^4 - 2h^2y_j^2 + 2h^2x_i^2.$$

Therefore

$$r^2_{i-1,j}\, r^2_{i+1,j}\, r^2_{i,j-1}\, r^2_{i,j+1} = [(x_i^2 + y_j^2 + h^2)^2 + 3h^4]^2 - 4h^4(x_i^2 - y_j^2)^2.$$

We develop the term and remark that

$$\left[(x_i^2 + y_j^2 + h^2)^2 + 3h^4\right]^2 - 4h^4(x_i^2 - y_j^2)^2 \geq (x_i^2 + y_j^2 + h^2)^4,$$

which gives us (16). The relationship (17) is directly obtained by using $x_i = y_j = 0$ in the first formula of the proof. □

The considered point P belongs to Ω_h^δ, thus the interface is at a distance bounded independently of h from P, and the function $\tilde{F}_P$ is C^2 with derivatives bounded independently of h on irregular grid points and interface points. Thus one can prove with Taylor expansions that there exist strictly positive constants C_2 and C_3 such that

$$-\Big(\nabla.(k\nabla\tilde{F}_P)\Big)^h_{i,j} \geq -C_2, \quad \forall\, M_{i,j} \in \Omega_h^*, \tag{18}$$

$$k_2(\partial_n\tilde{F}_P^2)^h_{i+1/2,j} - k_1(\partial_n\tilde{F}_P^1)^h_{i+1/2,j} \geq -C_3, \quad \forall\, I_{i+1/2,j} \in \Sigma_h, \tag{19}$$

$$k_2(\partial_n\tilde{F}_P^2)^h_{i,j+1/2} - k_1(\partial_n\tilde{F}_P^1)^h_{i,j+1/2} \geq -C_3, \quad \forall\, I_{i,j+1/2} \in \Sigma_h. \tag{20}$$

To sum up the previous lines, if we denote $\tilde{W}_P$ the array of the values of $\tilde{F}_P$ discretized on the grid and interface points, with $\tilde{W}_P \equiv 0$ on $\delta\Omega_h$, there exist three strictly positive constants, C_1, C_2 and C_3, such that

$$\begin{aligned}
&(A_h\tilde{W_P})(Q) \geq 0, \quad \forall Q \in \Omega_h \setminus \Omega_h^* \\
&(A_h\tilde{W_P})(P) \geq \frac{C_1}{h^2}, \\
&(A_h\tilde{W_P})(Q) \geq -C_2 \quad \forall Q \in \Omega_h^*, \\
&(A_h\tilde{W_P})(Q) \geq -C_3 \quad \forall Q \in \Sigma_h.
\end{aligned}$$

Therefore, we obtain for each point P belonging to Ω_h^δ

$$G_h(:,P) \leq \frac{h^2}{C_1}\tilde{W}_P(:) + h^2\frac{C_3}{C_1}\sum_{Q\in\Sigma_h} G_h(:,Q) + h^2\frac{C_2}{C_1}\sum_{Q\in\Omega_h^*} G_h(:,Q). \tag{21}$$

We want to sum this relationship for all points P belonging to Ω_h^δ. To this purpose we need to obtain an estimate of the sum of $\tilde{W}_P$ for all P belonging to Ω_h^δ.
Lets us consider any point $Q \in \Omega_h$. Because the isolines $\phi = \pm\delta$ have dimension 1, there exists an integer $M > 0$ independent of h, which is an upper bound of the number of points $P \in \Omega_h^\delta$ such that $ih \leq r_P(Q) \leq (i+1)h$. If we denote $N_\Omega = \lceil \frac{diam(\Omega)}{h} \rceil$, we thus can write:

$$\forall\, 1 \leq i \leq N_\Omega, \qquad card\Big(P, P \in \Omega_h^\delta, ih \leq r_P(Q) \leq (i+1)h\Big) \leq M,$$

Consequently, for all $Q \in \Omega_h$,

$$\begin{aligned}\sum_{P\in\Omega_h^\delta} \tilde{W}_P(Q) &= \sum_{P\in\Omega_h^\delta} \ln\Big(\frac{C}{r_P(Q)}\Big) \le M \sum_{i=1}^{N_\Omega} \ln\Big(\frac{C}{ih}\Big) \\ &\le \frac{M}{h} \sum_{i=1}^{N_\Omega} \int_{(i-1)h}^{ih} \ln\Big(\frac{C}{x}\Big) dx \\ &= \frac{M}{h} \underbrace{\int_0^{N_\Omega h} \ln\Big(\frac{C}{x}\Big) dx}_{=0(1)} = O(\frac{1}{h}).\end{aligned}$$

Using this result, if we sum the inequality (21) on all points in Ω_h^δ and use the estimate (14) for Σ_h, we obtain

$$\sum_{P\in\Omega_h^\delta} G_h(:,P) \le O(h) + O(h) \sum_{Q\in\Omega_h^*} G_h(:,Q). \tag{22}$$

- We define the function $\check{f}$ by :

$$\check{f}(x,y) = \begin{cases} B-1 & \text{if } |\phi(x,y)| \le h/2, \\ B - e^{A(|\phi(x,y)|-h/2)} & \text{if } h/2 \le |\phi(x,y)| \le \delta, \\ B - e^{A(\delta-h/2)} & \text{if } \delta \le |\phi(x,y)|, \end{cases}$$

with ϕ the signed distance to the interface, negative in Ω_2 and positive in Ω_1. This function is Lipschitz-continuous on the whole domain. It is also twice differentiable with bounded derivatives, excepted on the isolines of the level-set function $\phi = \pm\delta, \pm h/2$. Thus the discrete elliptic operator will be bounded for all grid points, excepted for the grid points in Ω_h^δ and grid points near the interface, including Ω_h^*, because the stencil for these points crosses these isolines.
The function $\check{f}$ satisfies for all (x,y) such that $h/2 < |\phi(x,y)| < \delta$:

$$-\Big(\nabla.(k\nabla\check{f})\Big)(x,y) = k\Big[A^2\Big(\underbrace{(\partial_x\phi)^2 + (\partial_y\phi)^2}_{=1}\Big) \pm A\nabla.(\nabla\phi)(x,y)\Big] e^{A(|\phi(x,y)|-h/2)},$$

because ϕ is the signed distance function. The sign $\pm$ in this formula depends on the subdomain to which (x,y) belongs. We choose A and B such that:

$$\begin{cases} kA^2 \pm A\nabla.(k\nabla\phi)(x,y) \ge 1, & \forall (x,y) \text{ such that } |\phi(x,y)| \le \delta, \\ \check{f}(x,y) \ge 0, & (x,y) \in \Omega. \end{cases}$$

For all regular grid points $M_{i,j}$ belonging to $\Omega_h \setminus \Omega_h^\delta$, with $|\phi(x_i,y_j)| < \delta$, we thus have:

$$-\left(\nabla.(k\nabla\check{f})\right)_{i,j}^{h} \geq 0. \tag{23}$$

On the other side, for all regular grid points $M_{i,j}$ belonging to $\Omega_h \setminus \Omega_h^\delta$, with $|\phi(x_i, y_j)| > \delta$, because the function $\check{f}$ is constant, we have

$$-\left(\nabla.(k\nabla\check{f})\right)_{i,j}^{h} = 0. \tag{24}$$

The function ϕ is Lipschitz continuous on grid points in Ω_h^δ, so there exists a strictly positive constant C_4 such that

$$-\left(\nabla.(k\nabla\check{f})\right)_{i,j}^{h} \geq -\frac{C_4}{h}, \quad \forall\, M_{i,j} \in \Omega_h^\delta. \tag{25}$$

Let us consider a grid point $M_{i,j}$ whose stencil for the elliptic operator crosses one of the isolines $|\phi| = h/2$. If $|\phi(M_{i,j})| \leq h/2$, then $\check{f}(M_{i,j}) = B - 1$. Thus the values of the other points involved in the stencil are smaller than $\check{f}(M_{i,j})$, meaning that $-\left(\nabla.(k\nabla\check{f})\right)_{i,j}^{h} \geq 0$. If $|\phi(M_{i,j})| > h/2$, then there is at least one point in the stencil satisfying $|\phi| < h/2$ and the value of $\check{f}$ on such a point is smaller than it would be if $\check{f}$ was not truncated at the value $B - 1$. Consequently, we have also in this case $-\left(\nabla.(k\nabla\check{f})\right)_{i,j}^{h} \geq 0$.

The discontinuity in the first derivative of $\check{f}$ on isolines $|\phi| = h/2$ is defined such that the discrete elliptic operator applied to $\check{f}$ on an irregular point will be computed with at least two first-order derivatives whose value differs by a $O(1)$ amplitude. Consequently, the discrete elliptic operator applied to $\check{f}$ on an irregular point will scale like $\dfrac{1}{h}$.

As a consequence of the previous lines, there exists a strictly positive constant C_5 such that

$$-\left(\nabla.(k\nabla\check{f})\right)_{i,j}^{h} \geq \frac{C_5}{h}, \quad \forall\, M_{i,j} \in \Omega_h^*. \tag{26}$$

Finally, the discrete normal derivative of $\check{f}$ computed with the formula involving points in Ω_2 (resp. Ω_1) is positive (resp. negative), therefore

$$k_2(\partial_n\check{f}^2)_{i+1/2,j}^{h} - k_1(\partial_n\check{f}^1)_{i+1/2,j}^{h} \geq 0, \quad \forall\, I_{i+1/2,j} \in \Sigma_h, \tag{27}$$

$$k_2(\partial_n\check{f}^2)_{i,j+1/2}^{h} - k_1(\partial_n\check{f}^1)_{i,j+1/2}^{h} \geq 0, \quad \forall\, I_{i,j+1/2} \in \Sigma_h. \tag{28}$$

Therefore, if we denote $\check{W}$ the array of the values of $\check{f}$ discretized on the grid and interface points, with $\check{W} \equiv 0$ on $\delta\Omega_h$, there exist strictly positive constants C_4 and C_5 such that

$$
\begin{aligned}
(A_h \tilde{W_P})(Q) &\geq 0, \quad \forall Q \in \Omega_h \setminus \Omega_h^{\delta}, \\
(A_h \tilde{W_P})(Q) &\geq -\frac{C_4}{h}, \quad \forall Q \in \Omega_h^{\delta}, \\
(A_h \tilde{W_P})(Q) &\geq \frac{C_5}{h}, \quad \forall Q \in \Omega_h^{*}, \\
(A_h \tilde{W_P})(Q) &\geq 0, \quad \forall Q \in \Sigma_h,
\end{aligned}
$$

and we conclude that

$$
\sum_{Q \in \Omega_h^*} G_h(:, Q) \leq \frac{C_4}{C_5} \sum_{Q \in \Omega_h^{\delta}} G_h(:, Q) + \frac{h}{C_5} \breve{W}(:). \tag{29}
$$

Combining (22) and (29) we obtain

$$
\sum_{Q \in \Omega_h^*} G_h(:, Q) \leq \frac{C_4}{C_5} \Big(O(h) + O(h) \sum_{Q \in \Omega_h^*} G_h(:, Q) \Big) + \frac{h}{C_5} \breve{W}(:).
$$

Therefore, for h small enough, we obtain:

$$
\sum_{Q \in \Omega_h^*} G_h(:, Q) \leq O(h). \tag{30}
$$

3.3.3 Convergence result

Finally, we obtain an estimate of the local error $e_h(P)$ on every point P in $\Omega_h \cup \Sigma_h$, with $\bar{u}$ the exact solution:

$$
\begin{aligned}
|e_h(P)| &= |\bar{u}(P) - u_h(P)| \\
&= \Big| \sum_{Q \in \Omega_h \cup \Sigma_h} G_h(P, Q) \tau(Q) \Big| \\
&\leq \Big| \sum_{Q \in \Omega_h^*} G_h(P, Q) \tau(Q) \Big| + \Big| \sum_{Q \in \Omega_h \setminus \Omega_h^*} G_h(P, Q) \tau(Q) \Big| + \Big| \sum_{Q \in \Sigma_h} G_h(P, Q) \tau(Q) \Big| \\
&\leq O(h) \Big| \sum_{Q \in \Omega_h^*} G_h(P, Q) \Big| + O(h^2) \Big| \sum_{Q \in \Omega_h \setminus \Omega_h^*} G_h(P, Q) \Big| + O(h) \Big| \sum_{Q \in \Sigma_h} G_h(P, Q) \Big| \\
&\leq O(h) O(h) + O(h^2) O(1) + O(h) O(1) = O(h)
\end{aligned}
$$

which proves that the numerical solution converges with first-order accuracy to the exact solution in L^{∞}-norm.

This computation allows to isolate the contribution of each different approximation errors. In particular, we can see that it is not necessary to have a first-order truncation error on the irregular points, but that an $O(1)$ truncation error would lead to the same order of convergence. We can also see that the convergence is limited to

first-order accuracy because of the first-order approximation of fluxes. If a second-order approximation of fluxes was used, we would obtain a global second-order convergence, provided that the resulting approximation matrix is monotone.

4 Convergence proof for the one-dimensional case

4.1 Monotonicity of the discretization matrix

Here we aim to prove that A_h is monotone in spite of the fact that the matrix A_h is not diagonally-dominant in the second-order version, due to the discretization terms near the interface.

Theorem 4 *Let v be an array of size $N + N_{int}$ corresponding to N grid points and N_{int} interface unknowns such that $A_h v \geq 0$, A_h being the discretization matrix corresponding of the method in one-dimension described in subsection 2.2. Then, all coefficients of v are non-negative.*

Proof. Let v be an array of size $N + N_{int}$ corresponding to N grid points and N_{int} interface unknowns such that $A_h v \geq 0$. Let us assume that the minimum of v is located on an interface point $x_{int} = x_{k+1/2}$.

We will prove that, with the notations and orientation of the normal defined on Figure 3, the left normal derivative at this interface point is negative and the right normal derivative at this interface point is positive. Once we have proven this property, the proof of monotonicity of the matrix is exactly the same as in two dimensions, so we will not re-write it.

The left normal derivative at x_{int} is discretized by

$$(\partial_n v^2)^h_{k+1/2} = \frac{3-2d}{(1-d)(2-d)h}(v_{k+1/2} - v_k) - \frac{1-d}{(2-d)h}(v_k - v_{k-1}).$$

By hypothesis $A_h v \geq 0$ hence

$$-\Big(\frac{v_{k+1/2} - v_k}{(1-d)h} - \frac{v_k - v_{k-1}}{h}\Big) \geq 0,$$

therefore

$$(\partial_n v^2)^h_{k+1/2} \leq \frac{2-d}{(1-d)(2-d)h}(v_{k+1/2} - v_k) \leq 0.$$

Moreover, if one can prove that the normal derivative is zero, then, with the last inequality, we can deduce that $v_k = v_{k+1/2}$. Similarly, the right normal derivative at $x_{k+1/2}$ is discretized by

$$(\partial_n v^1)^h_{k+1/2} = \frac{1+2d}{d(d+1)h}(v_{k+1} - v_{k+1/2}) - \frac{d}{(1+d)h}(v_{k+2} - v_{k+1}).$$

By hypothesis $A_h v \geq 0$ hence

$$-\Big(\frac{v_{k+2}-v_{k+1}}{h}-\frac{v_{k+1}-v_{k+1/2}}{dh}\Big)\geq 0,$$

therefore

$$(\partial_n v^1)^h_{k+1/2}\geq \frac{1+d}{d(d+1)h}(v_{k+1}-v_{k+1/2})\geq 0.$$

Again, if the normal derivative is zero, then $v_{k+1}=v_{k+1/2}$. □

4.2 Second-order convergence

With exactly the same reasoning than in subsection 3.3 we can prove the estimates (15), (14) and (22). We use them to obtain an estimate of the local error on every point P in $\Omega_h \cup \Sigma_h$:

$$\begin{aligned}
|e_h(P)| &= |\bar{u}(P)-u_h(P)| \\
&= \Big|\sum_{Q\in\Omega_h\cup\Sigma_h} G_h(P,Q)\tau(Q)\Big| \\
&\leq \Big|\sum_{Q\in\Omega_h^*} G_h(P,Q)\tau(Q)\Big| + \Big|\sum_{Q\in\Omega_h\setminus\Omega_h^*} G_h(P,Q)\tau(Q)\Big| + \Big|\sum_{Q\in\Sigma_h} G_h(P,Q)\tau(Q)\Big| \\
&\leq O(h)\Big|\sum_{Q\in\Omega_h^*} G_h(P,Q)\Big| + O(h^2)\Big|\sum_{Q\in\Omega_h\setminus\Omega_h^*} G_h(P,Q)\Big| + O(h^2)\Big|\sum_{Q\in\Sigma_h} G_h(P,Q)\Big| \\
&\leq O(h)O(h)+O(h^2)O(1)+O(h^2)O(1)=O(h^2)
\end{aligned}$$

which proves that the numerical solution converges with second-order accuracy to the exact solution in L^∞-norm.

5 Discussion

Numerous numerical methods have been developed for solving the problem (1) - (3), leading to a second-order accuracy in maximum norm, among them:

- the pioneering work of Mayo in 1984 [31], where an integral equation was derived to solve elliptic interface problems with piecewise coefficients. A second-order and fourth-order Cartesian grid-based boundary integral method for an interface problem of the Laplace equation on closely packed cells was also proposed recently in [37].

- the very well known Immersed Interface Method (IIM) of LeVeque and Li (1994) [25], and its developments, among them: the fast IIM algorithm of Li [28] for elliptic problems with piecewise constant coefficients, the Explicit Jump Immersed Interface Method (EJIIM) by Wiegmann and Bube [36], the Decomposed Immersed Interface Method (DIIM) by Bethelsen [5], and the MIIM (maximum principle preserving) by Li and Ito [29].
- the Matched Interface and Boundary (MIB) method [40], [39], [16], introduced by Zhou *et al.* : the solution on each side of the interface is extended on fictitious points on the other side. These fictitious values are computed by iteratively enforcing the lowest order interface jump conditions. This method can provide finite-difference schemes of arbitrary high order.
- the Coupling Interface Method, proposed by Chern and Shu [10], where the discretizations on each subdomain are coupled through a dimension by dimension approach using the jump conditions.
- Recently, Guittet *et al.* proposed in [20] to add degrees of freedom close to the interface and use a Voronoi partition centered at each of these points to discretize the equations in a finite volume approach. Doing so, they obtain a symmetric positive definite linear system and a second-order convergence of the solution.
- In the context of finite element methods, which is quite different from the methodology used here, numerous developments have also been done on cartesian grids, for instance [21].

Other classes of Cartesian methods also exist, only first order accurate for interface problems in the case of interface problems, but simpler to implement: Gibou *et al.* ([17], [18]). Let us also mention a new approach to solve a Dirichlet problem by a finite difference analog of the boundary integral equations, presented in [3]. In this paper, the double layer potential is thought as the solution of an interface problem similar to the one considered in this paper. A few works have also been devoted to higher order discretizations, for instance [27] where an alternative approach based on non-matching grids is developed, with a fourth order compact finite difference scheme at border grid points that connect two meshes.

Concerning the discretization requirements needed to get a second-order spatial convergence, it has been noted since the introduction of Cartesian grid methods that an $O(h)$ truncation error at the points near the interface is enough to get an $O(h^2)$ convergence in maximum norm if the discretization is second-order on the regular grid points. However, in the literature, only few works have been devoted to the study of the second-order convergence of Cartesian grid methods for interface problems.

For one-dimensional methods, Huang and Li performed in [22] a convergence analysis of the IIM, using non-negative comparison functions, and in [36] Wiegmann and Bube presented a proof of convergence for one-dimensional problems with piecewise constant coefficients, using a detailed analysis and identification of the coefficients of the matrices involved. In [23], a convergence proof was established in one-dimension for a variant of the method studied in this paper, applied in the context of electropermeabilization models. But this proof was based on a row by row analysis of the discretization matrix, in order to obtain estimates of the coefficients of the inverse matrix. This technique would not be tractable in two dimensions, due to

its complexity. Recently, in [38], a second-order convergence proof was established by Zheng and Sweidan for a boundary-value variant of the Ghost-Fluid method, both for the solution and its derivative.

For two-dimensional methods, Beale and Layton [2] proved in two-dimensions the second-order convergence for piecewise constant diffusion coefficients, using the fact that a grid function located near the interface can be written as the divergence of a function smaller in norm. In [26], Li *et al.* proved the second-order convergence, for the solution and its gradient, in the case of an augmented method, where the jump in the normal derivative of the solution is considered as an additional unknown. The interface problem was rewritten as a new PDE consisting in a leading Laplacian operator plus lower derivatives terms near the interface. With this reformulation it was possible to use the result of [2] to prove the convergence. Li and Ito proved in [29] the second-order convergence of their MIIM, using the maximum principle. The proof uses a technical condition related to the location of the interface with respect to the grid point that is not always satisfied. For a slightly different kind of problem, in [1] it was proven that the numerical solution of a convection diffusion equation with an interface could allow an $O(h)$ truncation error near the interface and still have a solution with uniform $O(h^2)$ accuracy, and first differences of uniform accuracy almost $O(h^2)$. Recently a second-order convergence in L^∞-norm was proved in [15] for a 3D method based on an extension of the 2D finite element-finite difference method for general three dimensional anisotropic elliptic interface problems.

In this paper, the proof is also based on a discrete maximum principle, but differs significantly from the proof in [29] because the discretization is not the same, notably due to the presence of interface unknowns, which makes the monotonicity of the matrix a crucial step in the proof, and lead to a different application of the discrete maximum principle. This result can be considered as a step toward the convergence proof of the second-order method presented in [12]. In future works, we aim to adapt the ideas presented here to the original method itself. The crucial point being to prove that a discrete maximum principle can be applied to the discretization matrix, two alternatives could be explored:

- One could prove that the discretization matrix for the original second-order method is monotone. Because the discretization matrix is not diagonally dominant, one would probably need to combine adequatly some elliptic inequalities for the nodes near the interface into the expression of the discrete normal derivative. It may also be necessary to modify the stencil of the flux, but still maintaining its second-order accuracy.
- One could also use the technique presented in [7], where non-monotone finite-difference methods are proven to satisfy a generalized local maximum principle, still leading to a convergence result.

Finally, we want to emphasize that the technique that we have used to obtain the bounds on the coefficients of the inverse matrix could also be used to prove the convergence of numerical methods for other numerical methods for elliptic problems, for instance without singular source terms but with discontinuous diffusion coefficients. Indeed, to our knowledge, classical estimates of the discrete Green

functions were obtained mainly for smooth diffusion coefficients k, like for instance in [6].

6 Numerical study

In this section we provide numerical results only for the first-order method in two dimensions, as the second-order method has already been validated in two-dimensions in [12]. This numerical study is not meant to assess performances of the method but simply to corroborate the analysis that we have performed.

In the following we consider a square domain Ω consisting in the union of two subdomains Ω_1 and Ω_2 separated by an interface Σ. We impose exact Dirichlet boundary conditions on the outer boundary of Ω.

6.1 Numerical study of the discrete Green functions

Here we study numerically the amplitude in L^∞-norm, of the different sums of discrete Green functions estimated in subsections 3.3.1 and 3.3.2. We consider an elliptical interface Σ defined as:

$$(\frac{x}{18/27})^2 + (\frac{y}{10/27})^2 = 1.$$

The amplitude in L^∞-norm of the sums of the different groups of discrete Green function is presented in Table 1. We observe the same behaviour as the estimates (15), (14) and (30), namely an $O(1)$ behaviour for $\sum_{Q\in\Sigma_h} G_h(P,Q)$ and $\sum_{Q\in\Omega_h} G_h(P,Q)$, and an $O(h)$ behaviour for $\sum_{Q\in\Omega_h^*} G_h(P,Q)$.

N	Σ_h	Ω_h	Ω_h^*
50	1.803×10^{-1}	2.985×10^{-1}	3.374×10^{-2}
100	1.817×10^{-1}	2.965×10^{-1}	1.5642×10^{-2}
200	1.818×10^{-1}	2.957×10^{-1}	8.371×10^{-3}
400	1.820×10^{-1}	2.952×10^{-1}	4.164×10^{-3}

Table 1 Numerical amplitude in L^∞-norm of the different groups of discrete Green functions.

6.2 Convergence study: problem 1

It is a test case appearing in [40] (MIB method, case 3 of the tests on irregular interfaces) and [10] (CIM, example 4). We consider an elliptical interface Σ defined as:

$$(\frac{x}{18/27})^2 + (\frac{y}{10/27})^2 = 1.$$

The exact solution is:

$$u(x,y) = \begin{cases} e^x \cos(y), \text{ inside } \Sigma, \\ 5e^{-x^2-\frac{y^2}{2}} \text{ otherwise.} \end{cases}$$

We set the diffusion coefficient $k = 1$ outside the interface, and $k = 10$ inside the interface. We compute the convergence order p by comparing the numerical errors $e(N_1)$ and $e(N_2)$ respectively computed with N_1 and N_2 number of grid points in each direction, with the formula:

$$p = \frac{\ln(\frac{e(N_1)}{e(N_2)})}{\ln(\frac{N_2}{N_1})}.$$

We observe a first-order convergence, as presented in Table 2.

N	L^∞ error	order
20	1.0521×10^{-1}	-
40	5.3019×10^{-2}	0.99
80	2.5699×10^{-2}	1.02
160	1.3015×10^{-2}	1.00
320	6.5679×10^{-3}	1.00

Table 2 Numericals results for Problem 1.

Moreover, we want to give a numerical evidence of the influence of the truncation error for the discretization of the elliptic operator on irregular points. To this purpose we add to the linear system used for the above test an additional source term uniformly equal to one to all lines of the linear system corresponding to the discretization of the elliptic operators for points in Ω_h^*. Then we check that the resulting order of convergence is unchanged. The resulting errors and numerical convergence order are displayed in Table 3. The amplitude of the L^∞ is higher, as expected, but we still observe a first-order convergence.

N	L^∞ error	order
20	3.2979×10^{-1}	-
40	1.9303×10^{-1}	0.77
80	8.5741×10^{-2}	0.97
160	4.3055×10^{-2}	0.98
320	2.2028×10^{-2}	0.98

Table 3 Numericals results for Problem 1 with a perturbation in $O(1)$ of source term for irregular points.

6.3 Convergence study: problem 2

It is a test case studied in [30]. We consider a spherical interface Σ defined by $r^2 = 1/4$ with $r = \sqrt{x^2 + y^2}$. The exact solution is:

$$u(x, y) = \begin{cases} e^x \cos(y) \text{ inside } \Sigma, \\ 0 \text{ otherwise.} \end{cases}$$

The numerical results and orders of convergence are presented in Table 4. We observe again a first-order convergence.

N	L^∞ error	order
20	4.9234×10^{-3}	-
40	2.2717×10^{-3}	1.12
80	1.0763×10^{-3}	1.10
160	5.5813×10^{-4}	1.05
320	2.4518×10^{-4}	1.08

Table 4 Numericals results for Problem 2.

Acknowledgements

The author wants to thank sincerely Zhilin Li, Juan Ruiz-Álvarez and the reviewers for their constructive and helpful comments.

References

1. J. T. Beale. Smoothing properties of implicit finite difference methods for a diffusion equation in maximum norm. *SIAM J. Numer. Anal.*, 47:2476–2495, 2009.

2. J. T. Beale and A. T. Layton. On the accuracy of finite difference methods for elliptic problems with interfaces. *Commun. Appl. Math. Comput. Sci.*, 1:91–119, 2006.
3. J. T. Beale and W. Ying. Solution of the dirichlet problem by a finite difference analog of the boundary integral equation. *Numer. Math.*, 141(3):605–626, March 2019.
4. M. Bergmann and L. Weynans. A sharp cartesian method for incompressible flows with large density ratios. Technical Report RR8926, INRIA Research Report, 2017.
5. P. Bethelsen. A decomposed immersed interface method for variable coefficient elliptic equations with non-smooth and discontinuous solutions. *J. Comput. Phys.*, 197:364–386, 2004.
6. J. H. Bramble and V. Thomee. Pointwise bounds for discrete Green's functions. *SIAM J. Numer. Anal.*, 6(4):583–590, 1969.
7. A. Brandt. Generalized local maximum principles for finite-difference operators. *Mathematics of Computations*, 27:685–718, 1973.
8. D. Bresch, T. Colin, E. Grenier, B. Ribba, and O. Saut. Computational modeling of solid tumor growth: the avascular stage. *SIAM J. Sci. Comput.*, 32:2321–2344, 2009.
9. M. Breton, F. Buret, L. Krahenbuhl, M. Leguebe, L. Mir, R. Perrussel, C. Poignard, R. Scorretti, and D. Voyer. Nonlinear steady-state electrical current modeling for the electropermeabilization of biological tissue. *IEEE Trans. on Mag.*, 51:1–4, 2015.
10. I. Chern and Y.-C. Shu. A coupling interface method for elliptic interface problems. *J. Comput. Phys.*, 225:2138–2174, 2007.
11. P. G. Ciarlet. Discrete maximum principle for finite-difference operators. *Aequationes Mathematicae*, 4:338–352, 1970.
12. M. Cisternino and L. Weynans. A parallel second order cartesian method for elliptic interface problems. *Commun. Comput. Phys.*, 12:1562–1587, 2012.
13. C. Dapogny and P. Frey. Computation of the signed distance function to a discrete contour on adapted triangulation. *Calcolo*, 49(3):193–219, 2012.
14. J. Dardé, N. Nasr, and L. Weynans. Immersed boundary method for the complete electrode model in electrical impedance tomography. *J. Comput. Phys.*, 487:112150, 2023.
15. B. Dong, X. Feng, and Z. Li. An l^∞ second order cartesian method for 3d anisotropic interface problems. *J. Comput. Appl. Math.*, 6:882–912, 2019.
16. W. Geng and S. Zhao. A two-component matched interface and boundary (mib) regularization for charge singularity in implicit solvation. *J. Comput. Phys.*, 351:25–39, 2017.
17. F. Gibou, R. P. Fedkiw, L.T. Cheng, and M. Kang. A second order accurate symmetric discretization of the Poisson equation on irregular domains. *J. Comput. Phys.*, 176:205–227, 2002.
18. F. Gibou and R.P. Fedkiw. A fourth order accurate discretization for the Laplace and heat equations on arbitrary domains, with applications to the Stefan problem. *J. Comput. Phys.*, 202:577–601, 2005.
19. D. Gilbard and N. Trudinger. *Elliptic Partial Differential Equations of Second Order*. Springer, 1998.
20. A. Guittet, M. Lepilliez, S. Tanguy, and F. Gibou. Solving elliptic problems with discontinuities on irregular domains – the Voronoi Interface Method. *Journal of Computational Physics*, 298:747 – 765, 2015.
21. R. Guo and T. Lin. A group of immersed finite-element spaces for elliptic interface problems. *IMA Journal of Numerical Analysis*, 39:482–511, 2019.
22. H. Huang and Z. Li. Convergence analysis of the immersed interface method. *IMA J. Numer. Anal.*, 19:583–608, 1999.
23. O. Kavian, M. Leguebe, C. Poignard, and L. Weynans. Classical electropermeabilization modelling at the cell scale. *J. Math. Biol.*, 68:235–265, 2014.
24. M. Leguebe, C. Poignard, and L. Weynans. A second-order cartesian method for the simulation of electropermeabilization cell models. *J. Comput. Phys.*, 292:114–140, 2015.
25. R. J. Leveque and L.Z. Li. The immersed interface method for elliptic equations with discontinuous coefficients and singular sources. *SIAM J. Numer. Anal.*, 31(4):1019–1044, 1994.
26. Z. Li, H. Ji, and X. Chen. Accurate solution and gradient computation for elliptic interface problems with variable coefficients. *SIAM J. Numer. Anal.*, 55:570–597, 2017.

27. Z. Li, K. Pan, and J. Ruiz-Alvarez. Stable high order fd methods for interface and internal layer problems based on non-matching grids. *J. Comput. Appl. Math.*, 96:1647–1674, 2024.
28. Z.L. Li. A fast iterative algorithm for elliptic interface problems. *SIAM J. Numer. Anal.*, 35:230–254, 1998.
29. Z.L. Li and K. Ito. Maximum principle preserving schemes for interface problems with discontinuous coefficients. *SIAM J. Sci. Comput.*, 23:339–361, 2001.
30. X.-D. Liu, R. Fedkiw, and M. Kang. A boundary condition capturing method for Poisson's equation on irregular domains. *J. Comput. Phys.*, 160:151–178, 2000.
31. A. Mayo. The fast solution of Poisson's and the biharmonic equations on general regions. *SIAM J. Numer. Anal.*, 21:285–299, 1984.
32. S. Osher and R. Fedkiw. *Level Set Methods and Dynamic Implicit Surfaces*. Springer, 2003.
33. S. Osher and J. A. Sethian. Fronts propagating with curvature-dependent speed: Algorithms based on Hamilton-Jacobi formulations. *J. Comput. Phys.*, 79(12), 1988.
34. J. A. Sethian. *Level Set Methods and Fast Marching Methods*. Cambridge University Press, Cambridge, UK, 1999.
35. J. A. Sethian. Evolution, implementation, and application of level set and fast marching methods for advancing fronts. *J. Comput. Phys.*, 169:503–555, 2001.
36. A. Wiegmann and K. Bube. The explicit jump immersed interface method: finite difference method for PDEs with piecewise smooth solutions. *SIAM J. Numer. Anal.*, 37(3):827–862, 2000.
37. W. Ying. A cartesian grid-based boundary integral method for an elliptic interface problem on closely packed cells. *Commun. Comput. Phys.*, 24:1196–1220, 2018.
38. X. Zheng and M. Sweidan. Analysis of ghost-fluid method with cubic extrapolation for two-point boundary value problem. *IJNMA*, 18:19–58, 2019.
39. Y. C. Zhou and G. W. Wei. On the fictitious-domain and interpolation formulations of the matched interface and boundary (MIB) method. *J. Comput. Phys.*, 219:228–246, 2006.
40. Y. C. Zhou, S. Zhao, M. Feig, and G. W. Wei. High order matched interface and boundary method for elliptic equations with discontinuous coefficients and singular sources. *J. Comput. Phys.*, 213:1–30, 2006.